NASA TECHNICAL MEMORANDUM

NASA TM X-52767

NASA TM X-52767

NUMERICAL SOLUTION OF UNSTEADY FLOW IN A RECTANGULAR CAVITY WITH A MOVING WALL

by Leo F. Donovan
Lewis Research Center
Cleveland, Ohio

TECHNICAL PAPER proposed for presentation at Third Joint American Institute of Chemical Engineers - Instituto Mexicano de Ingenieras Quimicos Meeting Denver, Colorado, August 30 - September 2, 1970

NUMERICAL SOLUTION OF UNSTEADY FLOW IN A RECTANGULAR CAVITY WITH A MOVING WALL

by Leo F. Donovan

Lewis Research Center
Cleveland, Ohio

TECHNICAL PAPER proposed for presentation at

Third Joint American Institute of Chemical Engineers - Instituto Mexicano de Ingenieras Quimicos Meeting
Denver, Colorado, August 30 - September 2, 1970

NATIONAL AERONAUTICS AND SPACE ADMINISTRATION

NUMERICAL SOLUTION OF UNSTEADY FLOW IN A RECTANGULAR CAVITY WITH A MOVING WALL

by Leo F. Donovan

Lewis Research Center
National Aeronautics and Space Administration
Cleveland, Ohio

ABSTRACT

Unsteady flow in a two-dimensional, rectangular cavity with the upper wall moving at constant velocity is investigated. A numerical solution of the Navier-Stokes equations is used in which a Poisson's equation is solved iteratively for pressure and then velocities are calculated explicitly. The calculations start with the fluid at rest in the cavity and continue until no further changes in velocity occur. The aspect ratio of the cavity and the Reynolds number of the flow are the parameters of interest.

Results for cavities with aspect ratios of 1/2, 1, and 2 are presented for a Reynolds number of 100. For a square cavity, results are also given for several Reynolds numbers between 100 and 500.

Since the velocities calculated from the unsteady Navier-Stokes equations ultimately become steady at large times, they may be compared to velocities calculated from the steady Navier-Stokes equations or the results of steady experiments. This has been done where possible and generally satisfactory agreement is shown.

E-5577

TM X-52767

The unsteady results are illustrated by showing velocity profiles and three-dimensional plots of the pressure field at several times during the development of the flow for a Reynolds number of 500 in a square cavity. The paths of the instantaneous position of the vortex centers are also shown for all cases considered.

The unsteady results are also presented in an accompanying 16 mm movie in which marked particles are used to show the development of the flow. Selected frames of the movie are reproduced in the paper to illustrate this method of data presentation.

INTRODUCTION

The flow in a two-dimensional rectangular cavity with a moving wall gives rise to several aspects of fluid behavior that are of interest: accelerating and decelerating portions of the flow, stagnation and separation, and vortex formation. This problem is of interest in bearing and seal studies, is difficult to study experimentally without disturbing the flow, and is interesting in its own right. Time exposure photographs have been taken (1, 2) of such flows into which a tracer has been injected, so that the qualitative features of the steady flow are known. Figure 1 illustrates the circulatory motion of the fluid for a square cavity. For cavities with aspect ratios (i.e., depth/width) of one or less, most of the fluid rotates about a point - the vortex center - where the vector velocity is zero. Near the center of the vortex the flow is essen-

tially inviscid and velocity varies linearly with distance from the vortex center. However, in the outer portion of the vortex, viscosity cannot be ignored. The main vortex occupies most of the cavity but small, weak, counterrotating vortices exist in both lower corners. For a cavity with an aspect ratio of two, Figure 2 illustrates that there is an additional large, weak, counter-rotating vortex occupying most of the lower portion of the cavity.

Two features, in addition to the experimental and analytical difficulties due to the complicated nature of the flow, tend to make a numerical solution of this cavity flow problem attractive, namely, the geometry is simple and no fluid enters or leaves the cavity so that the boundary conditions are easily satisfied. Solutions of the steady Navier-Stokes equations have been reported (1, 3, 4, 5, 6, 7, 8); unsteady flow in a square cavity has also been solved numerically, but only steady results were presented in Reference 9.

The technique devised by Harlow (10) for calculating free surface flows was modified and used in Reference 11 to solve the problem of unsteady flow in a square cavity at a Reynolds number of 100. The calculations were carried out until velocities were no longer changing, at which point they were in excellent agreement with an extant numerical solution of the steady Navier-Stokes equations. In addition, the terminal position of the unsteady vortex center agreed well with the position of a vortex center estimated from a time exposure photograph of a steady vortex.

The object of the present paper is to extend the solution presented in Reference 11 to rectangular cavities and to higher Reynolds numbers. Comparisons are made where possible with numerical solutions of the steady Navier-Stokes equations and a vortex center position determined experimentally. The unsteady results are illustrated by presenting selected frames from a motion picture of the development of the flow, using special marked particles that move with the fluid and make it visible.

ANALYSIS

Differential Equations

The equations that describe the constant density, two-dimensional flow of interest are the continuity equation and (modified) Navier-Stokes equations for a Newtonian fluid.

$$\frac{\partial u}{\partial x} + \frac{\partial v}{\partial y} = 0 \tag{1}$$

$$\frac{\partial u}{\partial t} + \frac{\partial u^2}{\partial x} + \frac{\partial uv}{\partial y} = -\frac{\partial \varphi}{\partial x} + Re^{-1}\left[\frac{\partial^2 u}{\partial y^2} - \frac{\partial^2 v}{\partial x\, \partial y}\right] \tag{2}$$

$$\frac{\partial v}{\partial t} + \frac{\partial v^2}{\partial y} + \frac{\partial uv}{\partial x} = -\frac{\partial \varphi}{\partial y} + Re^{-1}\left[\frac{\partial^2 v}{\partial x^2} - \frac{\partial^2 u}{\partial x\, \partial y}\right] \tag{3}$$

where $Re = UL/\bar{\nu}$ is the Reynolds number and $\varphi = \bar{p}/\bar{\rho}U^2$ is a dimensionless pressure. The u- and v-components of velocity are in the x- and y-directions, respectively. The length and velocity of the moving wall, L and U, have been used to make these equations dimensionless.

Rather than convert to stream function and vorticity at this point, we have chosen to retain the primitive variables. Application of the boundary conditions is straightforward and extension to three-dimensions at a later date will be easier. We will seek an iterative solution to an equation for pressure obtained by differentiating the x- and y-momentum equations with respect to x and y, respectively, and adding the resulting equations. After some rearrangement one obtains a Poisson's equation for pressure

$$\frac{\partial^2 \varphi}{\partial x^2} + \frac{\partial^2 \varphi}{\partial y^2} = -\frac{\partial}{\partial t}\left(\frac{\partial u}{\partial x} + \frac{\partial v}{\partial y}\right) - \frac{\partial^2 u^2}{\partial x^2} - 2\frac{\partial^2 uv}{\partial x\, \partial y} - \frac{\partial^2 v^2}{\partial y^2} \qquad (4)$$

The first term to the right of the equality sign in Equation (4) is the time derivative of the left hand side of the continuity equation and, as such, should be zero. The reason for retaining this term will be discussed in a later section.

The initial condition and boundary conditions are straightforward. The fluid is at rest in the cavity at the start of the calculation so that initially the velocities are everywhere zero and the pressure is uniform. No-slip and impermeability boundary conditions require the velocities to vanish at the walls, except at the moving wall where the tangential component of velocity attains the constant wall velocity.

Finite Difference Representation

The positions of the variables on the finite difference mesh

are shown in Figure 3. The positions are chosen so that vertical walls pass through positions where the u-component of velocity is defined, horizontal walls pass through positions where the v-component of velocity is defined, and pressures are cell-centered. These positions have been chosen to facilitate application of the boundary conditions.

If it is necessary to evaluate one of the variables at a position where it is not defined, an average is used. For example,

$$u_{i,j} = \frac{1}{2}\left(u_{i,j+1/2} + u_{i,j-1/2}\right) \tag{5}$$

Centered differences are used to represent derivatives. For example,

$$\frac{\partial u_{i,j}}{\partial x} = \frac{1}{\delta x}\left(u_{i,j+1/2} - u_{i,j-1/2}\right) \tag{6}$$

When the derivative of a product of undefined quantities is formed, the product is differentiated and then averages are formed. For example, performing the differentiation first

$$\frac{\partial^2 (uv)_{i,j}}{\partial x\, \partial y} = \frac{1}{\delta x\, \delta y}\left[(uv)_{i+1/2,\, j+1/2} - (uv)_{i-1/2,\, j+1/2} - (uv)_{i+1/2,\, j-1/2} + (uv)_{i-1/2,\, j-1/2}\right] \tag{7}$$

and then averaging

$$(uv)_{i+1/2,\, j+1/2} = \frac{1}{4}\left(u_{i+1,\, j+1/2} + u_{i,\, j+1/2}\right)\left(v_{i+1/2,\, j+1} + v_{i+1/2,\, j}\right) \tag{8}$$

Difference Equations

The implicit finite difference form of equation (4) is

$$\varphi_{i,j} = \frac{1}{2\left(\frac{1}{\delta x^2} + \frac{1}{\delta y^2}\right)} \left(\frac{\varphi_{i,j+1} + \varphi_{i,j-1}}{\delta x^2} + \frac{\varphi_{i+1,j} + \varphi_{i-1,j}}{\delta y^2} + r_{i,j} \right) \tag{9}$$

where

$$r_{i,j} = \frac{1}{\delta x^2} \left(u^2_{i,j+1} - 2u^2_{i,j} + u^2_{i,j-1} \right) + \frac{2}{\delta x\, \delta y} \left[(uv)_{i+1/2,\, j+1/2} - (uv)_{i-1/2,\, j+1/2} - (uv)_{i+1/2,\, j-1/2} + (uv)_{i-1/2,\, j-1/2} \right] + \frac{1}{\delta y^2} \left(v^2_{i+1,j} - 2v^2_{i,j} + v^2_{i-1,j} \right) + \frac{1}{\delta t} \left(d^{n+1}_{i,j} - d_{i,j} \right) \tag{10}$$

$$d^{n+1}_{i,j} = 0 \tag{11}$$

$$d_{i,j} = \frac{1}{\delta x} \left(u_{i,j+1/2} - u_{i,j-1/2} \right) + \frac{1}{\delta y} \left(v_{i+1/2,j} - v_{i-1/2,j} \right) \tag{12}$$

The $d_{i,j}$ are the correction terms from the previous time $(n)\delta t$ and reflect the fact that the continuity equation was satisfied only approximately. The time derivative of the correction term also involves $d^{n+1}_{i,j}$. However, since it is desired that the continuity equation be satisfied as closely as possible at the new time $(n+1)\delta t$, the $d^{n+1}_{i,j}$ are set to zero. If the correction terms were

not included in Equation (9) the pressure iteration would have to be carried further; this would require more computer time than the technique used here. Harlow and Hirt (12) discuss the use of the correction term in more detail.

The explicit finite difference forms of Equations (2) and (3) are

$$u^{n+1}_{i,\,j+1/2} = u_{i,\,j+1/2} + \delta t \left\{ -\frac{1}{\delta x}\left(u^2_{i,\,j+1} - u^2_{i,\,j}\right) \right.$$
$$- \frac{1}{\delta y}\left[(uv)_{i+1/2,\,j+1/2} - (uv)_{i-1/2,\,j+1/2}\right]$$
$$- \frac{1}{\delta x}\left(\varphi_{i,\,j+1} - \varphi_{i,\,j}\right) + Re^{-1}\left[\frac{1}{\delta y^2}\left(u_{i+1,\,j+1/2}\right.\right.$$
$$\left. - 2u_{i,\,j+1/2} + u_{i-1,\,j+1/2}\right) - \frac{1}{\delta x\,\delta y}\left(v_{i+1/2,\,j+1}\right.$$
$$\left.\left. \left. - v_{i+1/2,\,j} - v_{i-1/2,\,j+1} + v_{i-1/2,\,j}\right)\right]\right\} \qquad (13)$$

$$v^{n+1}_{i+1/2,\,j} = v_{i+1/2,\,j} + \delta t \left\{ -\frac{1}{\delta x}\left[(uv)_{i+1/2,\,j+1/2} - (uv)_{i+1/2,\,j-1/2}\right]\right.$$
$$- \frac{1}{\delta y}\left(v^2_{i+1,\,j} - v^2_{i,\,j}\right) - \frac{1}{\delta y}\left(\varphi_{i+1,\,j} - \varphi_{i,\,j}\right)$$
$$+ Re^{-1}\left[\frac{1}{\delta x^2}\left(v_{i+1/2,\,j+1} - 2v_{i+1/2,\,j} + v_{i+1/2,\,j-1}\right)\right.$$
$$\left.\left. - \frac{1}{\delta x\,\delta y}\left(u_{i+1,\,j+1/2} - u_{i,\,j+1/2} - u_{i+1,\,j-1/2} + u_{i,\,j-1/2}\right)\right]\right\}$$
$$(14)$$

Fictitious tangential velocities are defined 1/2 mesh spacing outside the cavity so that the interpolated value at the wall satisfies the no-slip boundary condition. For a stationary vertical wall at j-1/2,

$$v_{i-1/2,\,j-1} + v_{i-1/2,\,j} = 0 \qquad \text{for all } i \tag{15}$$

The normal velocity component at this wall can be written directly as

$$u_{i,\,j-1/2} = 0 \qquad \text{for all } i \tag{16}$$

Similarly, for a stationary horizontal wall at i-1/2,

$$u_{i-1,\,j-1/2} + u_{i,\,j-1/2} = 0 \qquad \text{for all } i \tag{17}$$

$$v_{i-1/2,\,j} = 0 \qquad \text{for all } i \tag{18}$$

The initial pressure is chosen to be unity. Thereafter the reference point for pressure (where a value of unity is maintained) is the center of the wall opposite the moving wall. Fictitious pressures 1/2 cell outside the cavity are defined since they are needed in the solution of Equation (9) for cells bordering the inside of the cavity. In order to solve Equation (9) it is necessary to know the fictitious pressures outside the cavity. The Navier-Stokes equations can be evaluated at the walls to provide this information since the normal component of velocity is always zero at a wall. For a left wall at j+1/2 Equation (13) can be written as

$$\varphi_{i,\,j} = \varphi_{i,\,j+1} + \frac{2\mathrm{Re}^{-1}}{\delta y}\left(v_{i+1/2,\,j+1} - v_{i-1/2,\,j+1}\right) \tag{19}$$

For a bottom wall at $i+1/2$ Equation (14) can be written as

$$\varphi_{i+1,\,j} = \varphi_{i,\,j} + \frac{2Re^{-1}}{\delta x}\,(u_{i,\,j+1/2} - u_{i,\,j-1/2}) \qquad (20)$$

The velocities are known, either from the initial condition or the previous time cycle.

Marked Particles

The traditional way of presenting the results of experimental or numerical fluid mechanical investigations is not the best way of helping one form a coherent, overall picture of a complicated flow situation; this is especially true if the flow is unsteady. Flow visualization experiments, in which a tracer is introduced into the fluid to make its movement visible, have been designed to overcome this difficulty in the laboratory. A numerical analogue of a flow visualization experiment offers the same advantages for numerical fluid dynamics studies. The technique devised by Fromm and Harlow (13) that uses a microfilm recorder to photograph marked particles displayed on a cathode ray tube serves this purpose.

An initial uniform distribution of one particle per cell is created in the fluid. Thereafter, these particles are moved with velocities appropriate to their location and time. The distance a particle is moved is simply the product of the velocity at its current location and the time interval over which that velocity is assumed to exist (i.e., the time step in the solution of the Navier-

Stokes equations). The u- and v-components of the velocity of a particle are the weighted averages of the velocities at the four closest mesh points at which those velocities are defined. Since u and v velocities are defined at different mesh locations, velocities at eight mesh locations will be involved in the movement of one particle. The weight assigned to a mesh point velocity is inversely proportional to its distance from the particle in question. Figure 4 shows this schematically for a typical particle.

An exception to this rule of particle movement occurs when a particle is within half a mesh spacing of a wall. It was found in Reference 11 that a better representation of a particle velocity in a boundary layer along a surface is obtained by using only the two mesh points within the cavity in calculating the tangential velocity component.

Solution Technique

The computer code to solve the equations was written in FORTRAN IV. The solution is accomplished by starting from the initial conditions and stepping forward in time, as follows:

1. At some current time $(n)\delta t$ solve Equation (9) using successive overrelaxation (14) to obtain the new pressure field. We have used a relaxation factor of 1.8 without any attempt at optimization. The iteration is continued until the field converges to some desired degree. We have found that the criterion suggested by Harlow (10),

$$\frac{|\varphi_q - \varphi_{q-1}|}{|\varphi_q| + |\varphi_{q-1}| + u_{i,j}^2 + v_{i,j}^2} < 2\times10^{-4} \qquad (21)$$

where a subscript q indicates the q^{th} iteration, is satisfactory.

2. Increase the time to $(n+1)\delta t$ and solve Equations (13) and (14) for the new velocities.

3. Check to see that the continuity equation is satisfied sufficiently closely; following Harlow (10), we make sure that each $d_{i,j}$ is smaller in absolute value than 3.5×10^{-3}.

4. Calculate and store the new positions of the particles.

5. Store any information from this time step that will be needed for print outs or data plots.

This procedure is repeated as long as necessary.

Since the new velocities are calculated explicitly, the time step is limited by stability conditions. Hirt (15) has suggested approximate criteria

$$Re^{-1} > \frac{1}{2}\,\delta t\, u^2 \qquad (22)$$

and

$$Re^{-1} > \frac{1}{2}\,\delta x^2\,\frac{\partial u}{\partial x}$$

where u is the average maximum fluid speed and $\partial u/\partial x$ is the average maximum velocity gradient in the direction of flow. For example, the first criterion indicates a time step of about 0.02 for Reynolds number of 100. Equal space increments of 0.05 were used to give a 20×20 mesh and it was observed that the second

criterion was satisfied also. The same space and time increments were also found to be satisfactory for Reynolds numbers at least as large as 500, indicating that the stability criteria are somewhat conservative for this cavity flow. Some of the calculations were also performed with time and space increments halved and essentially the same results were obtained.

About 1/2 minute of IBM System/360 Model 67 computer time was required per dimensionless time t regardless of Reynolds number for a square cavity. However, longer runs were necessary to reach steady conditions at larger Reynolds numbers. The criterion of steady conditions we have used is that the position of the vortex center change less than 1 percent over a period of 5 dimensionless time units. For a Reynolds number of 100 this occurred at about a dimensionless time of 10; for a Reynolds number of 500, it was not reached until about a dimensionless time of 25. Twice as many points were used for cavities of aspect ratio 1/2 or 2 and about twice as long a running time as for the square cavity was needed.

A 35 mm microfilm recorder is used to record output at the completion of a run. For each time step an outline of the cavity and the positions of the particles are plotted on a high precision cathode ray tube. For the square cavity, about 0.2 minute of computer time per dimensionless time is required for this with a time step of 0.02; for the cavities with aspect ratio of 1/2 or 2,

this time is doubled since twice as many points are involved.

The microfilm recorder is also used to prepare plots of data. We make plots of the path of the instantaneous position of the vortex center, two velocity traverses through the vortex center, and a three-dimensional plot of the pressure field.

DISCUSSION OF RESULTS

Aspect Ratio of 1/2, Reynolds Number of 100

Figure 5 shows a time exposure photograph (1) of a steady vortex from which the position of the vortex center can be estimated. Figure 6 compares this estimate with the position calculated by Zuk and Renkel (8) from the steady Navier-Stokes equations and the position determined from the unsteady Navier-Stokes equations at large times. The numerical solutions are in good agreement with each other and in fair agreement with the experimental value. The path of the instantaneous position of the vortex center is also shown; it starts under the midpoint of the moving wall, shifts downstream (i. e., in the direction of movement of the wall) and into the cavity, and turns upstream slightly to attain its terminal position.

Figures 7 and 8 compare terminal velocities from the solution of the unsteady Navier-Stokes equations with velocities calculated from the steady Navier-Stokes equations (8). The comparisons are shown as velocity traverses through the vortex center; Figure 7 shows velocity parallel to the moving wall in the

vertical traverse and Figure 8 shows velocity perpendicular to the moving wall in the horizontal traverse. In both figures the agreement is good.

Aspect Ratio of 2, Reynolds Number of 100

There are two large vortices when the aspect ratio of the cavity is 2. Figure 9 compares the terminal positions of both vortex centers calculated from solutions of the steady and unsteady Navier-Stokes equations at large times. The authors of Reference 8 calculated the steady care for comparison with the unsteady result. The numerical solutions are in good agreement with each other; no experimental value is available for comparison. The path of the instantaneous position of the upper vortex center is also shown and is similar to the path for cavities with aspect ratio of 1/2.

Figures 10 through 13 compare traverses of terminal velocities calculated from the unsteady Navier-Stokes equations with velocities calculated from the steady Navier-Stokes equations. The agreement between the solutions is good. Figures 10 and 11 are traverses through the upper vortex center. It can be seen that the flow in the upper part of the cavity is similar to the flow in the cavity with aspect ratio of 1/2 shown in Figures 7 and 8. Figures 12 and 13 are traverses through the lower vortex center. The flow in the lower part of the cavity is much slower (about two orders of magnitude) than in the upper part.

Square Cavity

Figure 14 shows a time exposure photograph (1) of a steady vortex in a square cavity at a Reynolds number of 100 from which the position of the vortex center can be estimated. Figure 15 compares this estimate with the positions determined from two numerical solutions of the steady Navier-Stokes equations (5, 8) and the unsteady Navier-Stokes equations of large times. The agreement among these various methods is excellent. The path of the instantaneous position of the vortex center is also shown; it is similar to the paths for cavities with aspect ratios of 1/2 and 2.

Figures 16 and 17 compare terminal velocities from the solution of the unsteady Navier-Stokes equations with velocities calculated from the steady Navier-Stokes equations (8). The curves, showing traverses through the vortex center, are similar to those already presented for a cavity with aspect ratio of 1/2. The agreement between the solutions is excellent. The flow in this square cavity is similar to the flows in the cavity with aspect ratio of 1/2 and the upper part of the cavity with aspect ratio of 2.

Figures 18 and 19 show how the velocity traverse through the vortex center changes as Reynolds number is increased from 200 to 400. Inspection of these figures shows that an increasing Reynolds number increases the extent of the inviscid portion of the flow about the vortex center. The only prior calculation

available for comparison (5), a vertical traverse from a solution of the steady Navier-Stokes equations at Reynolds number of 400, shows good agreement in Figure 20 with the solution of the unsteady Navier-Stokes equations at large times.

Figures 21 and 22 show velocity traverses through the vortex center for Reynolds number of 500 at various times. It can be seen that at successively larger times the inviscid portion of the flow occupies progressively larger fractions of the cavity.

Figure 23 shows three-dimensional plots of the pressure fields for Reynolds number of 500 and the same times as the velocity traverses shown in Figures 21 and 22. At the upper left corner of the cavity the pressure is below the reference pressure. The pressure rises along the moving wall, reaching a value about 40 percent greater than the reference pressure near the upper right corner on the last frame. A local minimum, about 8 percent below the reference pressure, exists at the vortex center. The pressure fields for lower Reynolds numbers were similar to those shown in Figure 23, but the minimums and maximums along the moving wall were more pronounced.

Figure 24 shows the effect of Reynolds number on the positions of the unsteady vortex centers as well as the terminal positions of the vortex centers for several Reynolds numbers from 100 to 500. It can be seen that increasing the Reynolds number shifts the terminal position of the vortex center upstream and

farther into the cavity. These positions fall quite close to the asymptote from linear theory (5), shown as the line drawn from the center of the cavity to the moving wall. The path of the instantaneous vortex centers moves farther downstream before turning down and upstream as Reynolds number increases.

Marked Particle Plots

Selected frames from the movie of flow in a cavity with aspect ratio of 2 at a Reynolds number of 100, chosen to illustrate the marked particle plots, are given in Figure 25. The first frame shows the initial uniform distribution of particles at rest at the start of the calculation. Succeeding frames show the development of the flow at dimensionless times of 1, 2, 3, 4, and 10. The small triangle above the cavity is used to show the velocity of the moving wall in the movie.

The circulatory nature of the flow is evident in these figures even though it is seen much more dramatically in the movies. The effect of the moving wall can be seen to propagate into the cavity with time. The lower portion of the cavity remains relatively quiescent, even at a dimensionless time of 10. Later frames show the beginnings of the development of the weak vortices.

CONCLUDING REMARKS

Unsteady flow in a two-dimensional, rectangular cavity with a moving wall was investigated by numerically solving the Navier-

Stokes equations. The calculations started with the fluid at rest in the cavity and continued until no further changes in velocity occurred. Results for cavities with aspect ratios of 1/2, 1, and 2 were presented for a Reynolds number of 100. For a square cavity, results were also given for several Reynolds numbers between 100 and 500.

Flow in cavities with aspect ratios of 1/2 and 1, and in the upper part of a cavity with aspect ratio of 2, were similar at a Reynolds number of 100. This was true of the unsteady, as well as the steady, flow.

As the Reynolds number increased from 100 to 500 in a square cavity the inviscid portion of the flow occupied a progressively larger portion of the cavity. At all of these Reynolds numbers the inviscid portion of the flow about the vortex center increased during the initial period.

For a square cavity the path of the instantaneous position of the vortex center approached the downstream wall more closely with increasing Reynolds number, even though the terminal position of the vortex center moved closer to the upstream wall.

The unsteady results were also presented in an accompanying 16 mm movie in which marked particles were used to show the development of the flow. Selected frames of the movie were reproduced in the paper to illustrate this method of data presentation. A loan copy of the movie is available on request from the author.

NOTATION

d	correction term, equation (12)
i	subscript indicating vertical position
j	subscript indicating horizontal position
L	reference length (length of moving wall)
n	superscript denoting n^{th} time step
Re	Reynolds number, $LU/\overline{\nu}$
r	abbreviation, equation (10)
t	time, $\overline{t}U/L$
U	reference velocity (velocity of moving wall)
u	velocity in x-direction, $\overline{u}/U$
v	velocity in y-direction, $\overline{v}/U$
x	horizontal direction, $\overline{x}/L$
y	vertical direction, $\overline{y}/L$

A dimensional quantity is denoted by an overbar or capital letter

Greek letters:

δt	time step
δx, δy	space increments
$\overline{\nu}$	kinematic viscosity of fluid
$\overline{\rho}$	density of fluid
φ	pressure, $\overline{p}/\overline{\rho}U^2$

LITERATURE CITED

1. Mills, R. D., J. Roy. Aeron. Soc., 69, 714 (1965).
2. Pan, F., and A. Acrivos, J. Fluid Mech., 28, 643 (1967).
3. Kawaguti, M., J. Phys. Soc. Japan, 16, 2307 (1961).
4. Weiss, R. F., and B. H. Florsheim, Phys. Fluids, 8, 1631 (1965).
5. Burggraf, O. R., J. Fluid Mech., 24, 113 (1966).
6. Runchal, A. K., D. B. Spalding, and M. Wolfshtein, Imperial College of Science and Technology, SF/TN/2 (August 1967).
7. Greenspan, D., Computer J., 12, 88 (1969).
8. Zuk, J. and H. E. Renkel, Paper No. FICFS-30 presented at the Fourth International Conference on Fluid Sealing, Philadelphia, Pa. (May 8, 1969).
9. Greenspan, D., P. C. Jain, R. Manohar, B. Noble, and A. Sakurai, Proceedings of the ARO Working Group on Computers, Harry Diamond Laboratories (1965).
10. Welch, J. E., F. H. Harlow, J. P. Shannon, and B. J. Daly, Los Alamos Sci. Lab., LA-3425 (March 21, 1966).
11. Donovan, L. F., To be published in AIAA J.
12. Hirt, C. W., and F. H. Harlow, J. Computational Phys., 2, 114 (1968).
13. Fromm, J. E., and F. H. Harlow, Phys. Fluids, 6, 975 (1963).

14. Varga, R. S., "Matrix Iterative Analysis," Prentice-Hall, Englewood Cliffs (1962).

15. Hirt, C. W., J. Computational Phys., 2, 339 (1968).

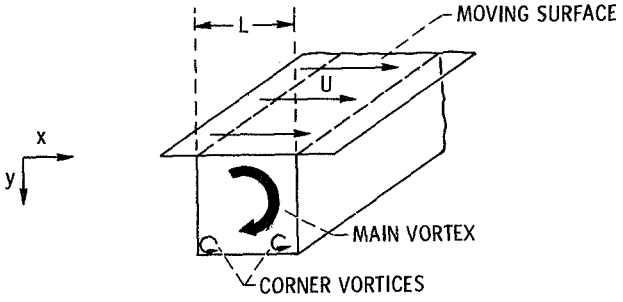

Figure 1. - Schematic diagram of square cavity.

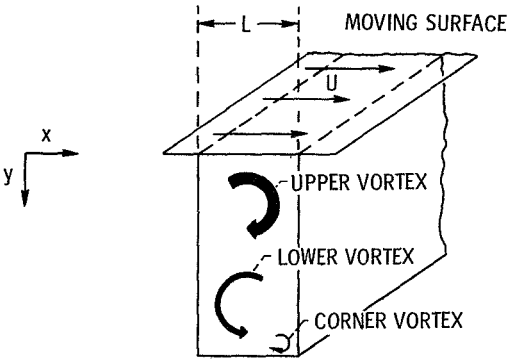

Figure 2. - Schematic diagram of cavity with aspect ratio of 2.

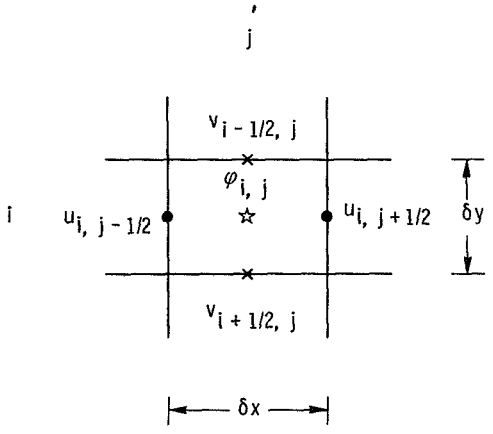

Figure 3. - Position of variables on finite difference mesh.

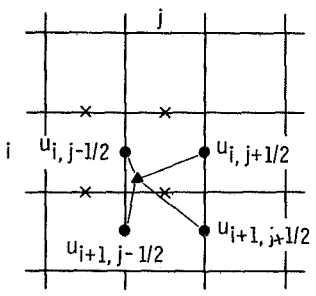

(A) u-VELOCITY COMPONENT.

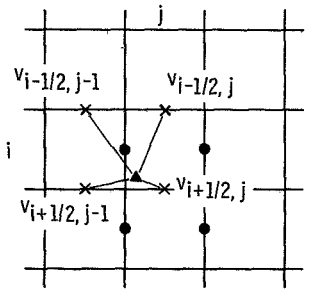

(B) v-VELOCITY COMPONENT.

Figure 4. - Mesh point velocities used to calculate particle velocity.

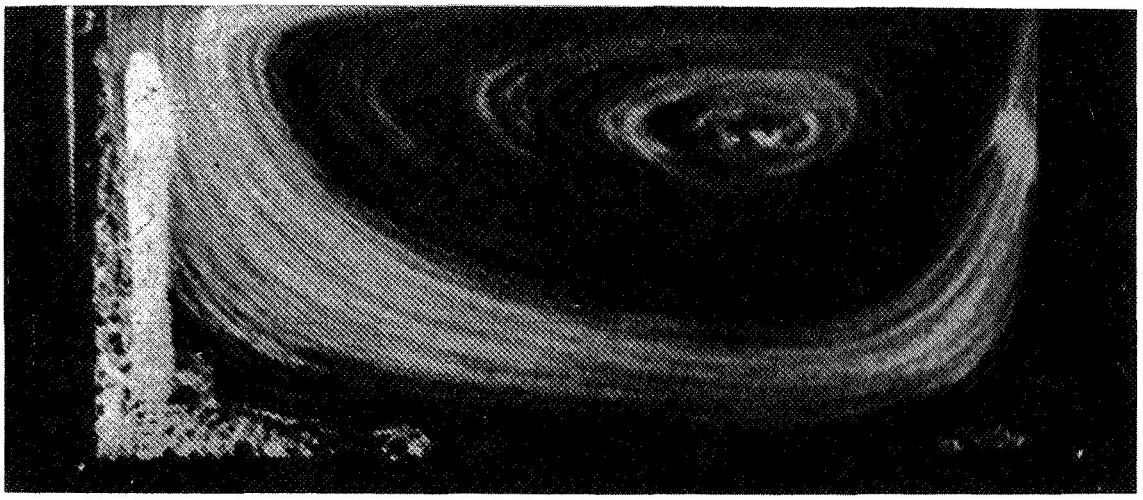

Figure 5. - Time exposure photograph of vortex in cavity of aspect ratio 1/2. Reynolds number = 100 (Ref. 1).

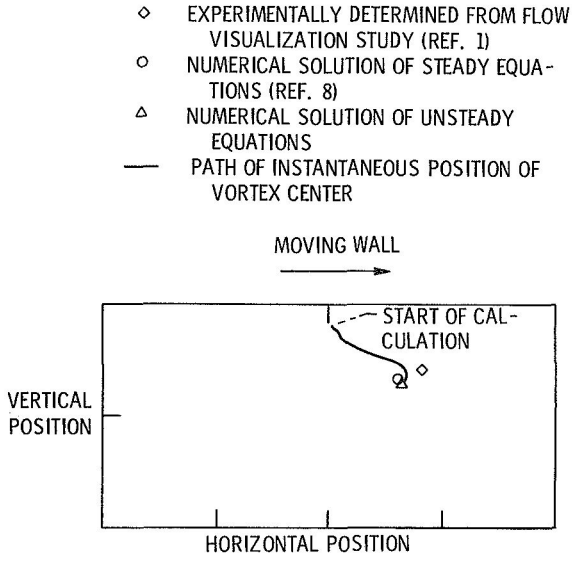

Figure 6. - Position of vortex center in cavity of aspect ratio of 1/2. Reynolds number = 100.

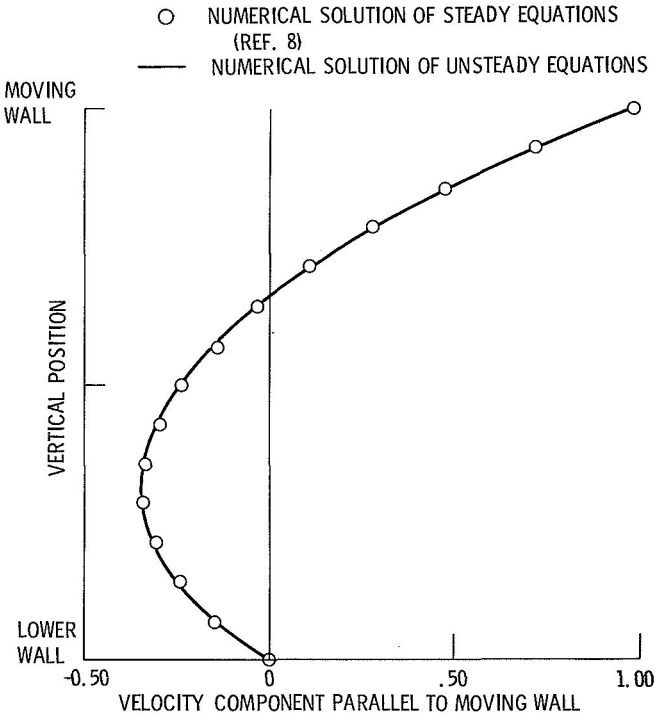

Figure 7. - Vertical velocity traverse through vortex center in cavity of aspect ratio 1/2. Reynolds number = 100.

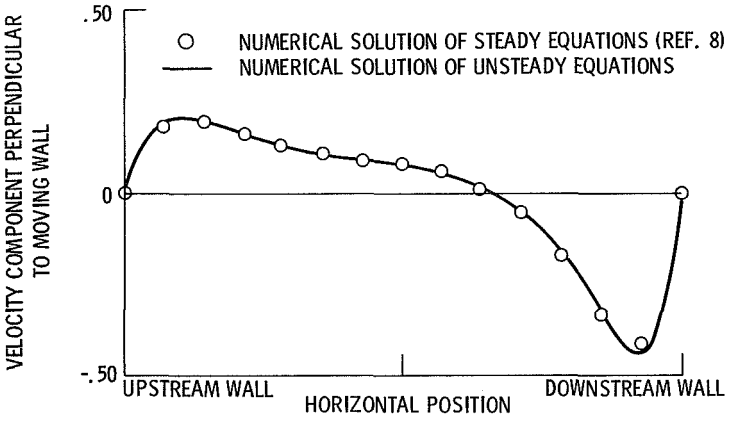

Figure 8. - Horizontal velocity traverse through vortex center in cavity of aspect ratio 1/2. Reynolds number = 100.

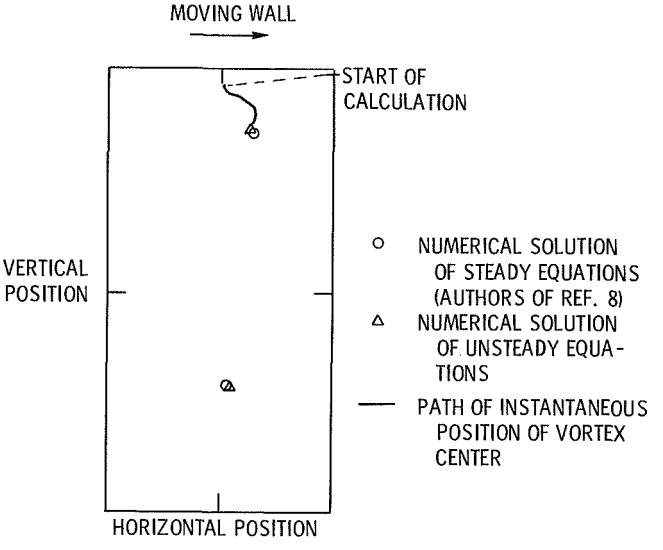

Figure 9. - Position of vortex centers in cavity of aspect ratio of 2. Reynolds number = 100.

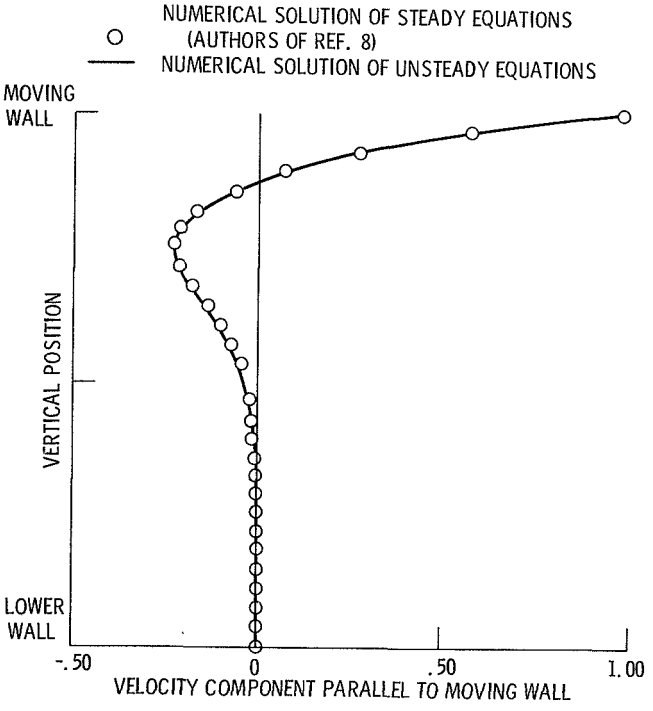

Figure 10. - Vertical velocity traverse through upper vortex center in cavity of aspect ratio 2. Reynolds number = 100.

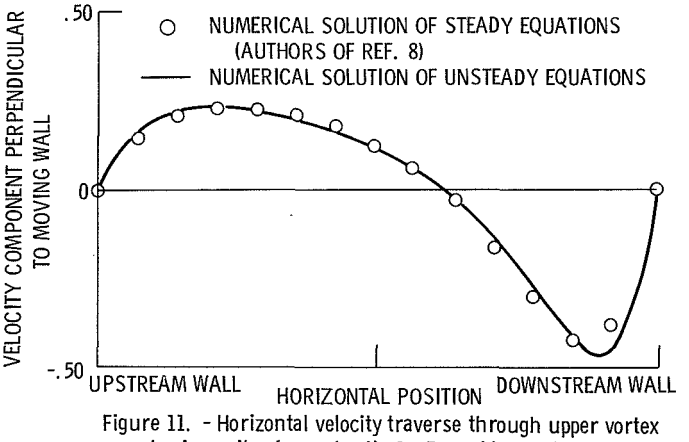

Figure 11. - Horizontal velocity traverse through upper vortex center in cavity of aspect ratio 2. Reynolds number = 100.

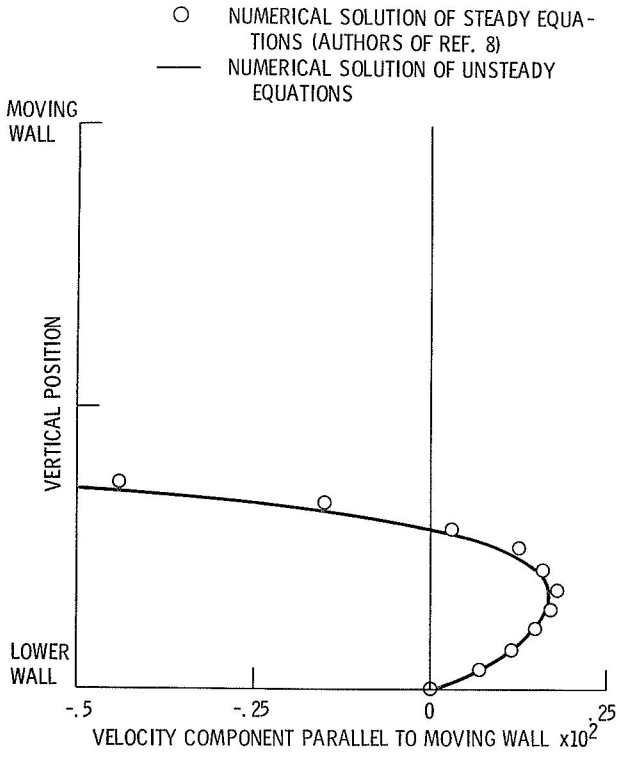

Figure 12. - Vertical velocity traverse through lower vortex center in cavity of aspect ratio 2. Reynolds number = 100.

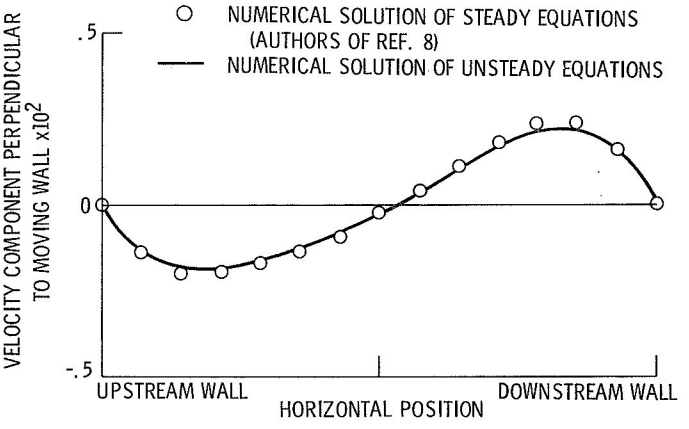

Figure 13. - Horizontal velocity traverse through lower vortex center in cavity of aspect ratio 2. Reynolds number = 100.

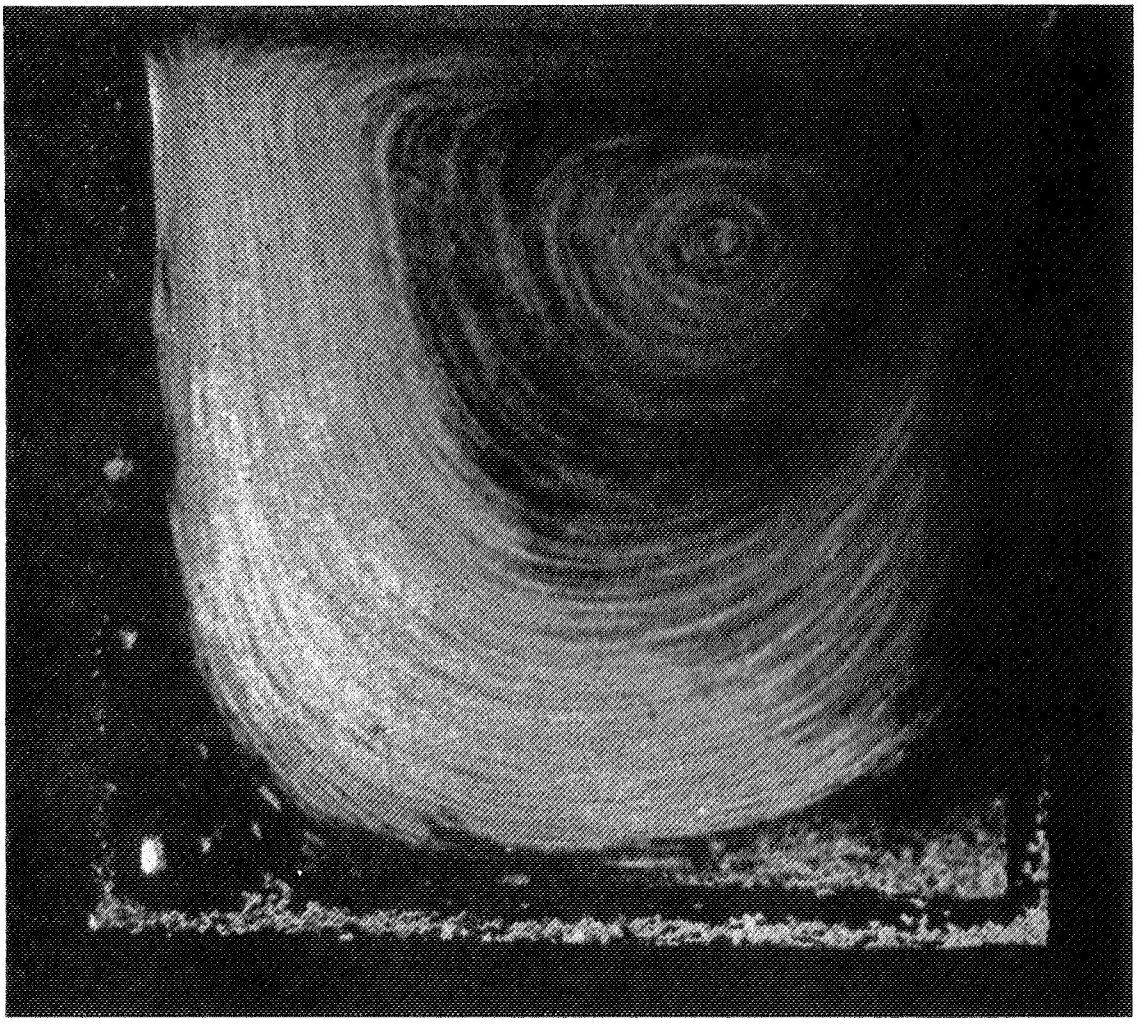

Figure 14. - Time exposure photograph of vortex in square cavity. Reynolds number = 100 (Ref. 1).

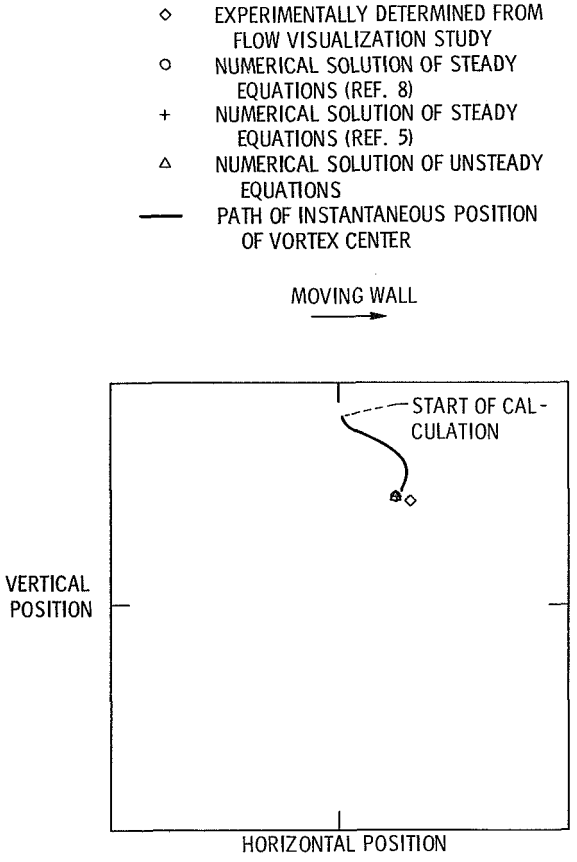

Figure 15. - Position of vortex center in square cavity. Reynolds number = 100.

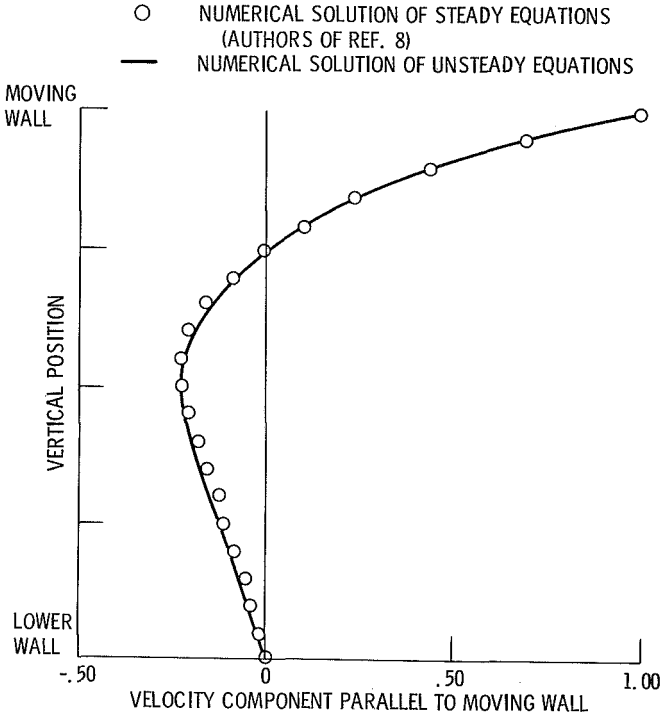

Figure 16. - Vertical velocity traverse through vortex center in square cavity. Reynolds number = 100.

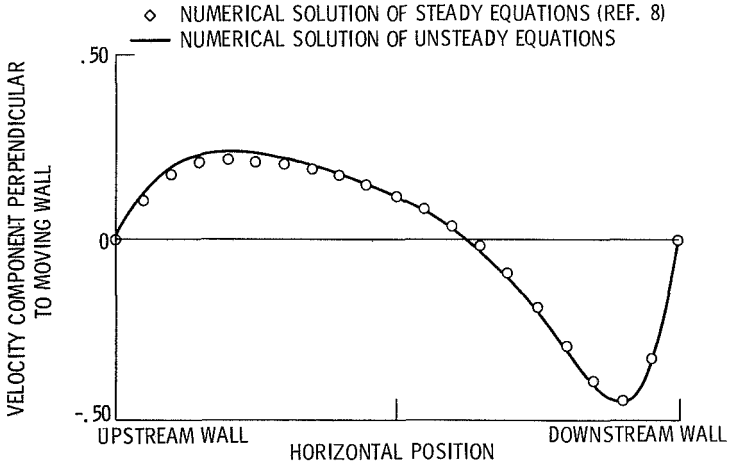

Figure 17. - Horizontal velocity traverse through vortex center in square cavity. Reynolds number = 100.

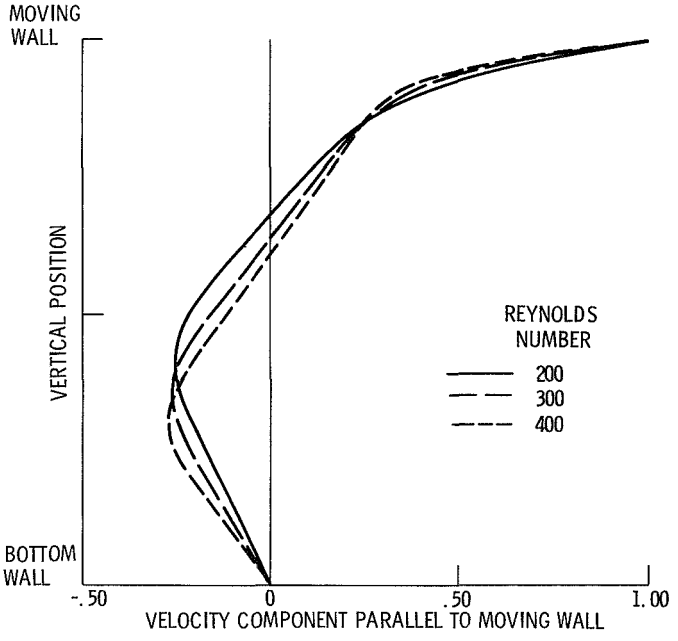

Figure 18. - Vertical velocity traverse through vortex center in square cavity.

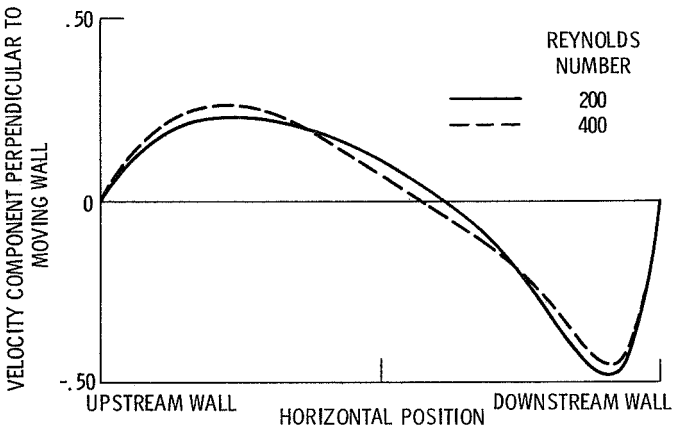

Figure 19. - Horizontal velocity traverse through vortex center in square cavity.

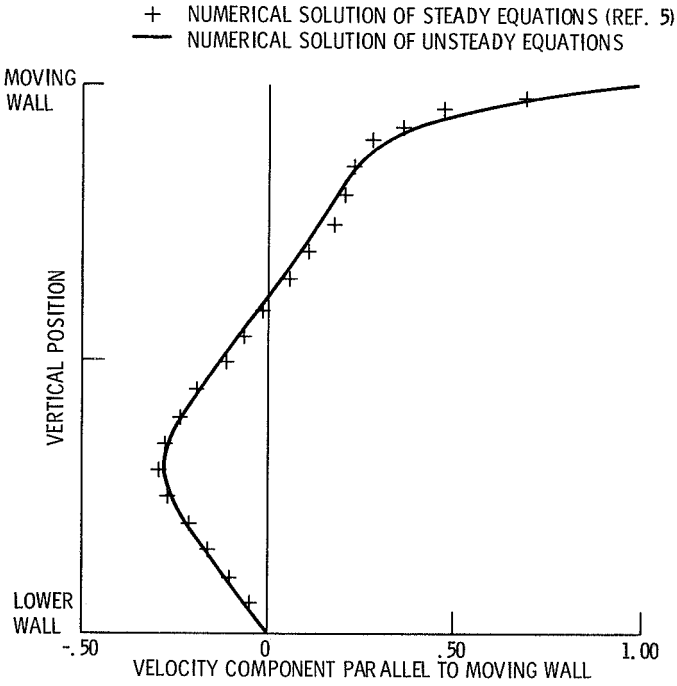

Figure 20. - Vertical velocity traverse through vortex center in square cavity. Reynolds number = 400.

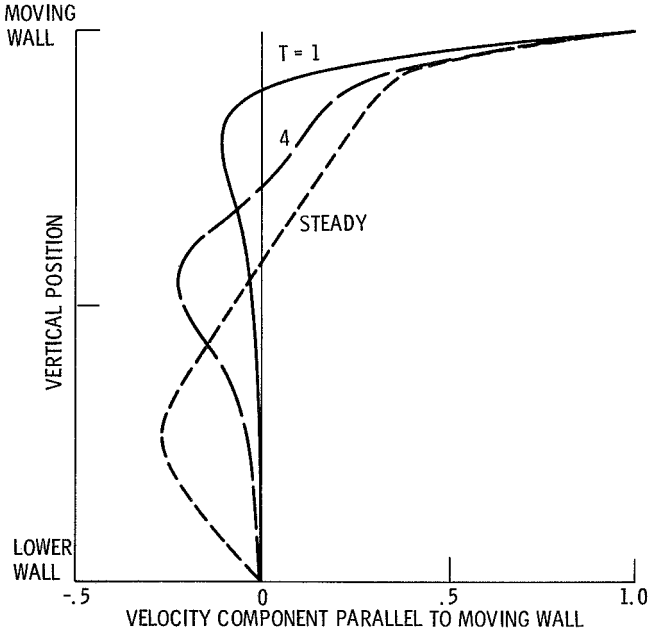

Figure 21. - Vertical velocity traverses through vortex centers in square cavity. Reynolds number = 500.

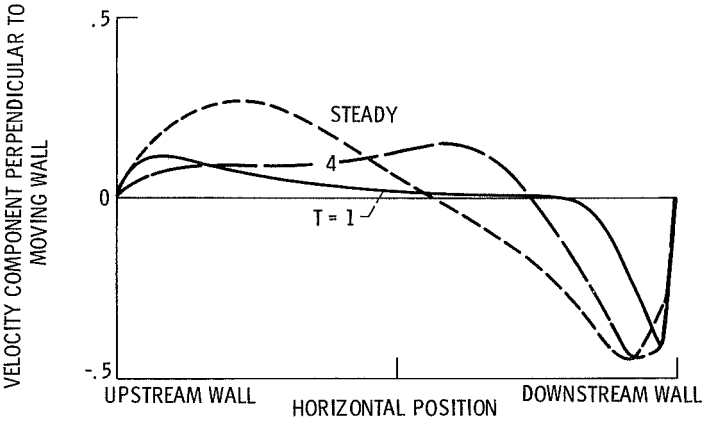

Figure 22. - Horizontal velocity traverses through vortex centers in square cavity. Reynolds number = 500.

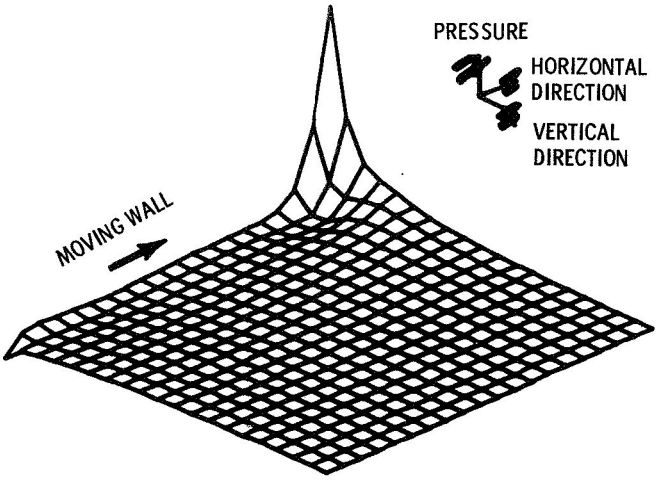

(a) Time = 1.

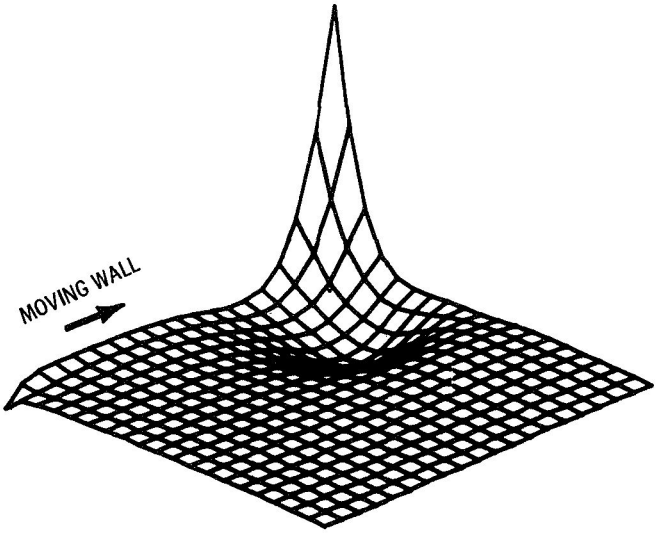

(b) Time = 4.

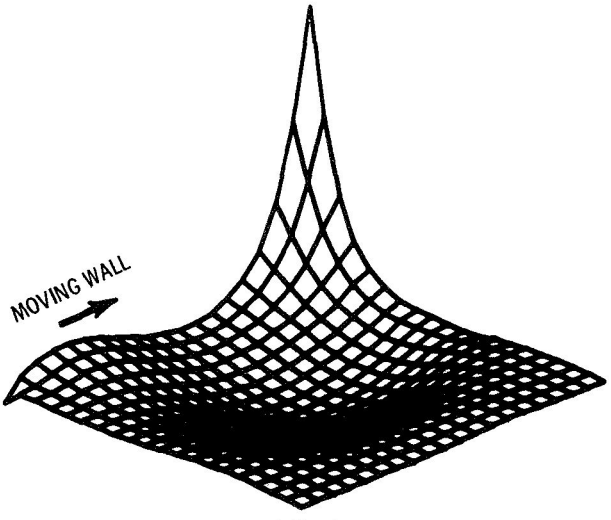

(c) Steady.

Figure 23. - Pressure distribution in square cavity. Reynolds number = 500.

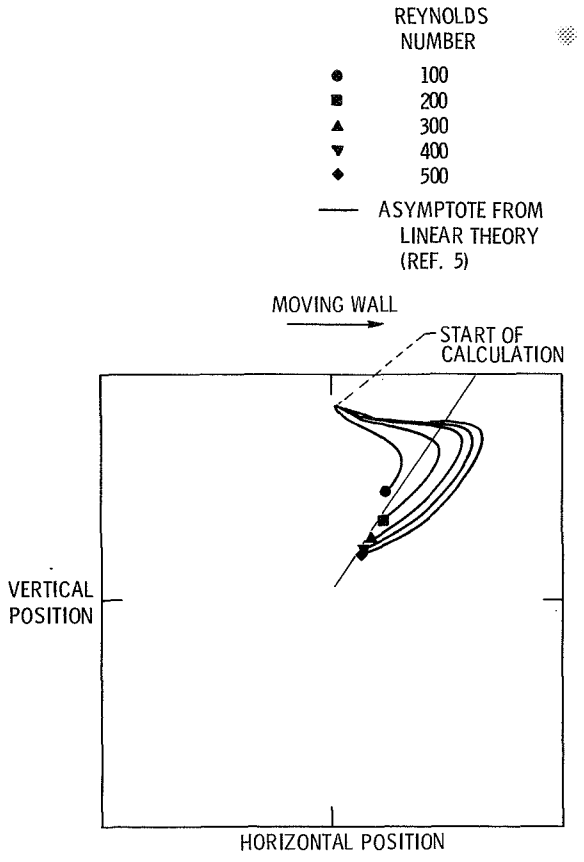

Figure 24. - Path of instantaneous position of vortex centers in square cavity.

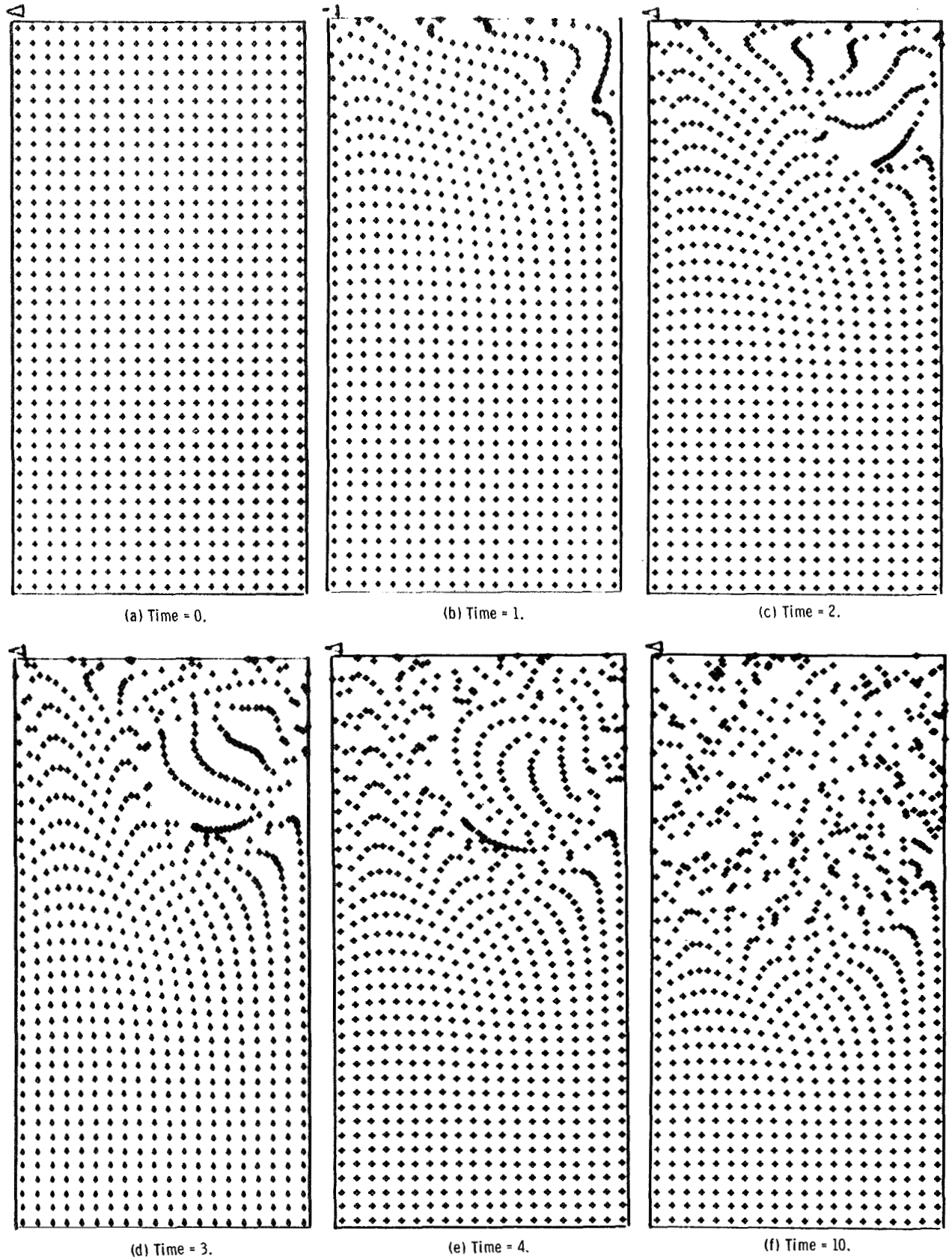

(a) Time = 0. (b) Time = 1. (c) Time = 2.

(d) Time = 3. (e) Time = 4. (f) Time = 10.

Figure 25. - Marked particle plots. Aspect ratio of 2. Reynolds number = 100.